Biosensors and Bioelectronics 71 (2015) 37–43

Contents lists available at ScienceDirect

Biosensors and Bioelectronics

journal homepage: www.elsevier.com/locate/bios

Surface charge modulated aptasensor in a single glass conical nanopore

Sheng-Lin Cai, Shuo-Hui Cao, Yu-Bin Zheng, Shuang Zhao, Jin-Lei Yang, Yao-Qun Li *

Department of Chemistry and the MOE Key Laboratory of Spectrochemical Analysis & Instrumentation, College of Chemistry and Chemical Engineering, Xiamen University, Xiamen 361005, China

ARTICLE INFO

Article history:
Received 23 September 2014
Received in revised form
6 March 2015
Accepted 4 April 2015
Available online 8 April 2015

Keywords:
Single glass conical nanopores
Surface charge neutralization
Ionic current
Aptamer
Protein sensing

ABSTRACT

In this work, we have proposed a label-free nanopore-based biosensing strategy for protein detection by performing the DNA–protein interaction inside a single glass conical nanopore. A lysozyme binding aptamer (LBA) was used to functionalize the walls of glass nanopore via siloxane chemistry and negatively charged recognition sites were thus generated. The covalent modification procedures and their recognition towards lysozyme of the single conical nanopore were characterized via ionic current passing through the nanopore membrane, which was measured by recording the current–voltage (*I*–*V*) curves in 1 mM KCl electrolyte at pH=7.4. With the occurring of recognition event, the negatively charged wall was partially neutralized by the positively charged lysozyme molecules, leading to a sensitive change of the surface charge-dependent current–voltage (*I*–*V*) characteristics. Our results not only demonstrate excellent selectivity and sensitivity towards the target protein, but also suggest a route to extend this nanopore-based sensing strategy to the biosensing platform designs of a wide range of proteins based on a charge modulation.

1. Introduction

The transport of ions and molecules regulated by biological ion channels are of great importance in various cellular and biological processes (Hille 1978; Hucho and Schiebler, 1977; Perozo et al., 2002). Biological nanopores such as α-hemolysin have been widely researched in the applications for analysis of nucleic acids (Clarke et al., 2009; Hurt et al., 2009; Wang et al., 2011b), proteins (Madampage et al., 2010; Wang et al., 2011a; Ying et al., 2012; Zhao et al., 2009), and small molecules (Howorka and Siwy, 2009; Wu and Bayley, 2008). However, such protein based nanopores together with their embedding lipid bilayers are unstable, fragile and impressionable to the external environments (Ali et al., 2010; Tahir et al., 2013; Tian et al., 2013). These drawbacks make them unsuitable for practical applications. Recently, solid-state nanopores have been rapidly developed with the advantages over their biological counterparts in terms of stability, robustness, and control over pore shape, diameter and the pore surface properties (Ali et al., 2011; Gyurcsanyi, 2008; Hou et al., 2011). And the broad applications such as biosensing (Choi et al., 2006; Gyurcsanyi, 2008; Tian et al., 2012; Wei et al., 2012; Schibel and Ervin, 2014), DNA sequencing (Fologea et al., 2005; Lagerqvist et al., 2006; Yan and Xu, 2006), molecular separation (Martin et al., 2001; Savariar et al., 2008), and mimicry of biological channels (Hou et al., 2011; Hou and Jiang, 2009; Zhang et al., 2011, 2010), have been explored.

Until now, two basic methods including resistive-pulse sensing (Luan and Zhou, 2012; Niedzwiecki et al., 2010; Sexton et al., 2007, 2010) and ion-current rectification (Ali et al., 2011, 2012, 2010, 2008; Tian et al., 2013; Wang and Martin, 2008; Yusko et al., 2010; Zhao et al., 2013) have been proposed for target analysis via synthetic nanopores. For the resistive-pulse sensing technique: when a molecule or particle was driven through a nanopore of comparable size, an electrical signal can be measured under the influenced of an applied voltage (Dekker, 2007; Li et al., 2012). However, as described by Ali et al. (Ali et al., 2010), this technique faces the limitation when considering the fast molecule translocation and concomitant electronic noise in more practical applications.

On the other hand, due to their comparable pore diameter with the electric double layers and excess surface charge on the pore walls, synthetic conically-shape nanopores can behave the special ion transport property called ionic current rectification, showing nonlinear current voltage curves (Zhang et al., 2011; Zhao et al., 2013). Once a nanopore channel was fabricated, its shape was hard to change, so that the ionic rectified characteristics will be mainly determined by the surface chemical properties of the nanopore. The rectified properties of synthetic nanopores can be utilized for the label-free detection of various analytes based on the change of

* Corresponding author. Fax: +86 592 2185875.
E-mail address: yaoqunli@xmu.edu.cn (Y.-Q. Li).

http://dx.doi.org/10.1016/j.bios.2015.04.002
0956-5663/

charge polarity or density on the pore surface, induced by the recognition of target molecules. Generally, to construct a nanopore-based biosensing platform, it is essential to introduce a suitable functional group acting as the recognition site to the sensible tip side of the conical nanopores.

In recent years, nucleic acids that act as molecules for self-assembly of molecular nanostructure and also as a material for building machinelike nanodevices have become important building blocks for bottom-up nanotechnology (Krishnan and Simmel, 2011). Motivated largely by the rapid development of the DNA nanotechnology and nanopore technology, researchers have paid great efforts in integrating DNA molecules into the synthetic nanopore systems and achieved a number of nucleic-acid-based nanopore sensing elements (Actis et al., 2011; Fu et al., 2009; Liu et al., 2013; Tian et al., 2013). Martin and co-workers have reported a DNA-functionalized nanotube membrane which showed an ability to selectively recognize the single-base mismatch DNA strands (Harrell et al., 2004; Kohli et al., 2004). Ali et al. demonstrated the design and construction of peptide nucleic acid (PNA)-modified synthetic ion channels for the sequence specific detection of single-stranded DNA oligonucleotides (Ali et al., 2010). Recently, Jiang and co-workers have developed a series of DNA conformational transformation-based biomimetic nanochannels and paved the way for constructing nanopore gating of pH (Xia et al., 2008), potassium (Hou et al., 2009) and mercury(II) ions (Tian et al., 2013). However, the design and construction of robust and inexpensive nucleic acid-based nanofluidic devices for highly sensitive and selective detection of various target analytes still remains great challenges in life science and materials science.

Among the enormous nucleic acids libraries, aptamers are extremely promising components that can act as biospecific recognition site for a wide range of target molecules with advantages over traditional antibodies, such as stability, small size and chemical simplicity, ease of synthesis and the general availability for almost any given protein (Krishnan and Simmel, 2011; Xiao et al., 2013). The previous research concerning the design of nanopore-based aptasensing paradigms (Abelow et al., 2010; Actis et al., 2011; Ding et al., 2009; Rotem et al., 2012; Zhang et al., 2015) has mostly focused on the conformational change induced by binding events, causing a pore blockage for signal detection. However, the important property that conical nanopores are highly susceptible towards the surface charge received little attention in nanopore-based aptasensing design. It is worth noting that some aptamers such as lysozyme binding aptamer (LBA) could undergo recognition-induced reversal of the charge with a proper pH control. This property has been utilized for constructing electrochemical sensors using both electrochemical impedance spectroscopy (EIS) (Rodriguez et al., 2005) and cyclic voltammetric (CV) (Cheng et al., 2007) methods.

Herein, we demonstrated a proof-of-concept that aptamer–protein interaction induced neutralization of the surface charge in a single glass conical nanopore, accompanied by a decrease in the rectified currents, can be used to develop a nanopore-based biosensing platform for the detection of target proteins with high selectivity and sensitivity. The LBA was first introduced to the nanopore channels via a covalent modification process. At proper pH value, the aptamer strand was negatively charged while the lysozyme (pI=11) molecules were positively charged. The biospecific interaction between proteins and aptamers induced the partial neutralization of negative surface charge, which led to a sensitive change in the rectified ionic current of the single conical nanopores. The monitoring of covalent modification of LBA and the recognition events were characterized by recording the change of ionic current of the single conical nanopore.

2. Materials and methods

2.1. Chemicals and Materials

Prism glass capillary (outer diameter ~1.35 mm, inner diameter ~0.95 mm, Hirschmann, Germany), platinum wire (diameter 25 μm, from Alfa Aesar), Tungsten wire (0.25 mm, 99.95%, Alfa Aesar); Ferrocene (Fc, 99%, Alfa Aesar); Tetra-n-butylammonium hexafluorophosphate ($TBAPF_6$, 98%, Alfa Aesar), 3-aminopropyl-triethoxylsilane (APTES, 99%, Sigma-Aldrich), Glutaraldehyde (25% solution in water, Acros); Lysozyme (Boyun); BSA (97%, Boyun); Pepsin (Boyun); Cytochrome C (98.89%, Calbiochem); The lysozyme binding aptamer (LBA) was purchased from Shanghai Sangon Co., Ltd (Shanghai, China). The 42-mer aptamer used for functionalization was amino-terminated at its 5′ end, that is 5′-$(CH_2)_6$-ACT TAC GAA TTC ATC AGG GCT AAA GAG TGC AGA GTT ACT TAG-3′. The counterpart Control DNA strand was also a 42 base numbers with amino-terminated (Control DNA), 5′-$(CH_2)_6$-ACT ATA CGT GCA TAT ACA GCT AGA GAT GCT AGG AGT ACT ATG-3′.

2.2. Preparation of single glass conical nanopore channels

We prepared single glass conical nanopore channels from glass capillaries, according to the method reported by White and coworkers with slight modifications (Zhang et al., 2006). Firstly, a platinum wire was electrochemically etched in 15% $CaCl_2$ to obtain a sharpened tip (see SEM images of the Pt tips in Fig. S1a and b). Then, the sharpened tip was sealed into a glass capillary. Finally, the Pt wire sealed in glass was pulled out and etched in the boiled aqua regia solution for 4 h to obtain the single conical glass nanopore channels. The geometry of the nanopore channel was observed from the fluorescence image by injecting 1 μM Rhodamine B solution into the pore (Fig. S1c). The pore radius was determined by measuring the steady-state diffusion-limited current of the Pt disk electrode (Fig. S1d) prior to etching according to the Eq. (1) (Zhang et al., 2004, 2006). It has been demonstrated that the relative uncertainty in r is within 20% compared to the results obtained from SEM (Zhang et al., 2004).

$$i_d = 4nFDC_b r \quad (1)$$

where i_d is the steady-state limiting current of the nanodisk electrode measured in 5.0 mM Ferrocene and 0.1 M Tetra-n-butylammonium hexafluorophosphate acetonitrile solution, n is the number of electrons transferred per molecule, F is the Faraday constant, D is the diffusion coefficient (2.4×10^{-5} cm^2/s), C_b is bulk concentration of the redox molecule, and r is the radius of Pt nanodisk, respectively.

2.3. Immobilization of LBA onto the single glass conical nanopore surface

Fig. 1 shows the schematic diagram of the modification process of LBA to the glass nanopore through siloxane chemistry. Firstly, the nanopore channel was treated with piranha acid (concentrated H_2SO_4/ 30% H_2O_2, V:V=3:1, 80 °C, 30 min), followed by washing with ultrapure water and absolute ethanol to obtain clean silica hydroxyl group on the interior surface. Then 5% APTES in absolute ethanol was used to react with the interior pore surface for 30 min, followed by rinsing with absolute ethanol and baking at 120 °C for 30 min. Afterwards, the resulting nanopore channel was treated with 2.5% glutaraldehyde aqueous solution overnight, followed by rinsing with ultrapure water thoroughly. Finally, the tris (hydroxymethyl)aminomethane hydrochloride solution (Tris–HCl, 20 mM, pH=7.4, containing 100 mM NaCl, 5 mM $MgCl_2$) with 5′-

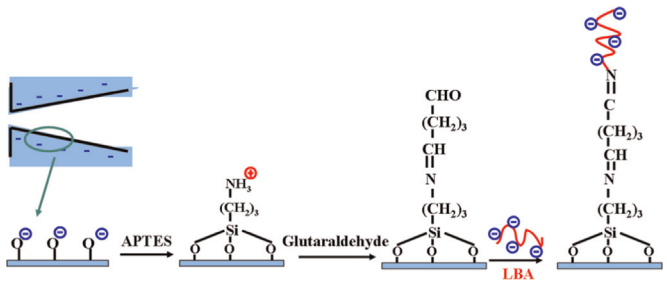

Fig. 1. Schematic description of the covalent modification procedures of glass nanopore surface with LBA.

aminated LBA (1 μM) was treated with the aldehyde groups terminated surface for ~20 h, followed by rinsing with Tris–HCl buffer solution and ultrapure water, respectively.

2.4. Current–voltage recording

Glass nanopore channels were filled with an aqueous 1 mM KCl solution prepared in phosphate buffer with pH=7.4 using a 100 μL microsyringe. An Ag/AgCl electrode (0.5 mm diameter) was inserted into the glass capillary and served as the working electrode, and another Ag/AgCl electrode (0.5 mm diameter) was placed in bulk solution as an auxiliary/reference electrode. In all cases, the nanopore channels were filled with the same electrolyte as the bulk solution. Linear sweep voltammetry experiments were carried out with a CHI 660C electrochemical workstation (Shanghai CHI Instrument Co. Ltd., China). The measurements of the resulting ion current flowing through the nanopore channel were performed by scanning the voltage from −1 V to +1 V with a scanning rate 100 mV/s. The error bars in each figure represent the measuring error of at least 3 independent measurements with the same nanopore. All measurements were performed at room temperature.

Various concentrations of lysozyme are prepared in the same electrolyte solution (1 mM KCl, pH=7.4), used for the measurement of respective *I–V* curve.

3. Results and discussion

3.1. Monitoring the modification of LBA

I–V characteristics of single glass conical nanopore were recorded in symmetric electrolyte conditions on both side of the nanopore. The rectification properties of the single conical nanopore were closely related to the surface charge polarity and density, just as demonstrated in other works (Siwy et al., 2004). Here, the *I–V* responses of the conical nanopore were employed to monitor the modification procedures. Fig. 2 shows the *I–V* curves of a single glass conical nanopore under each modification step. The unmodified single glass conical nanopore channel showed a nonlinear *I–V* curve in 1 mM KCl solution at pH=7.4; indicating the pore surface was negatively charged, due to the dissociation of the silica hydroxyl groups. After silanization, the amino groups were protonated at neutral condition, causing the pore walls to be positively charged. The *I–V* curves showed a reversal of the rectification direction. When the amino groups were further converted to aldehyde groups, almost linear *I–V* curve was recorded at pH=7.4. The loss of rectification reflects the presence of electrically neutral and reactive aldehyde groups on the surface. Upon immobilizing LBA, a significant increase in the ion current rectification was observed. This indicated that the pore walls were negatively charged, due to the fact that the DNA phosphate

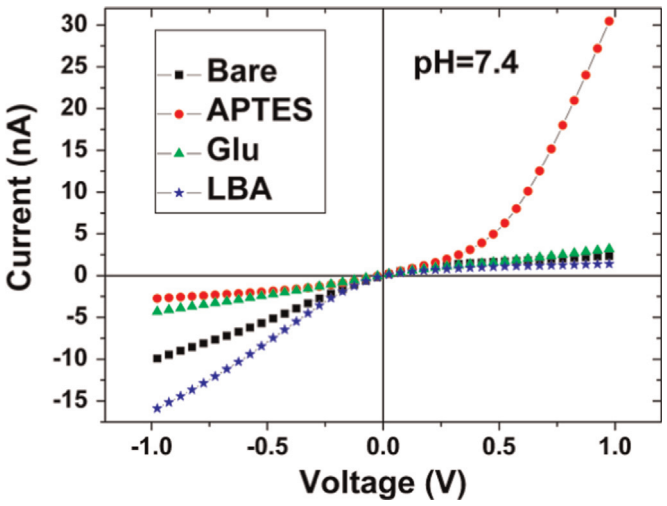

Fig. 2. Monitoring of the modification stages (silica hydroxyl groups ■, amino groups ●, aldehyde groups ▲, and immobilized aptamer strands ★, respectively) on the inner-surface of single glass conical nanopore channel by recording *I–V* curves in 1 mM KCl aqueous solution at pH=7.4. The tip radius is ~20 nm.

backbones were deprotonated at neutral condition. All the *I–V* curves in Fig. 2 helped us confirm the successful immobilization of LBA on the inner channel surface.

3.2. Sensing performance of the nanopore-based aptasensor

After preparing the novel aptamer-based nanodevice, we investigated the sensing performance of lysozyme by recording the current–voltage characteristics of the nanopore system prior to and after the addition of various concentrations of lysozyme in 1 mM KCl solution at pH=7.4. The LBA on the pore walls specifically recognized the lysozyme molecules in the bulk solution with rarely high affinity. Thus, the negative charges on the nanopore walls were subsequently partially neutralized by the positively charged lysozyme molecules (Fig. 3a), leading to a significant decrease on the rectified ionic current. Fig. 3b shows the variation of the *I–V* curves upon exposing the LBA-functionalized single glass conical nanopore channel to various concentrated lysozyme. As seen from Fig. 3b, upon the addition of a wide range of concentrations of lysozyme (from 0.5 pM to 10 nM), the ionic currents recorded at −1 V decreased dramatically, while the currents at +1 V stayed nearly the same, indicating that the decrease in rectification phenomenon of the nanopore.

Moreover, we employed the current-change ratio (R) at −1 V (defined as the absolute value of the current-change ratio, that is, $\Delta I/I_0$) to quantify the changes in the ionic current passing through the modified nanopore channels upon exposure to different concentrations of protein. Fig. 3c shows the current-change ratio at −1 V versus the additional lysozyme concentrations. The current-change ratio at −1 V firstly increased drastically when exposing the LBA-functionalized nanopore to low lysozyme concentrations from 0.5 to 10 pM, corresponding to ~7% and ~35% decreases at 0.5 and 10 pM, respectively. When the additional concentrations of lysozyme were further increased, the change of the current-change ratio tended to placid and finally stayed nearly the same (~50%) even the concentration was promoted to 10 nM. This may result from reaching saturation state of the nanopore in high concentration of lysozyme. Our experimental data of current-change ratio (R) versus logarithm concentration (lg C) was closely fit to the Langmuir model (Fig. 3c). Also we found a linear correlation exists between R and log C in the concentration range of 0.5–10 pM, that is R=0.219 lg C+0.129 with a regression correlation coefficient (r^2) of 0.973 (Fig. 3c inset). From the

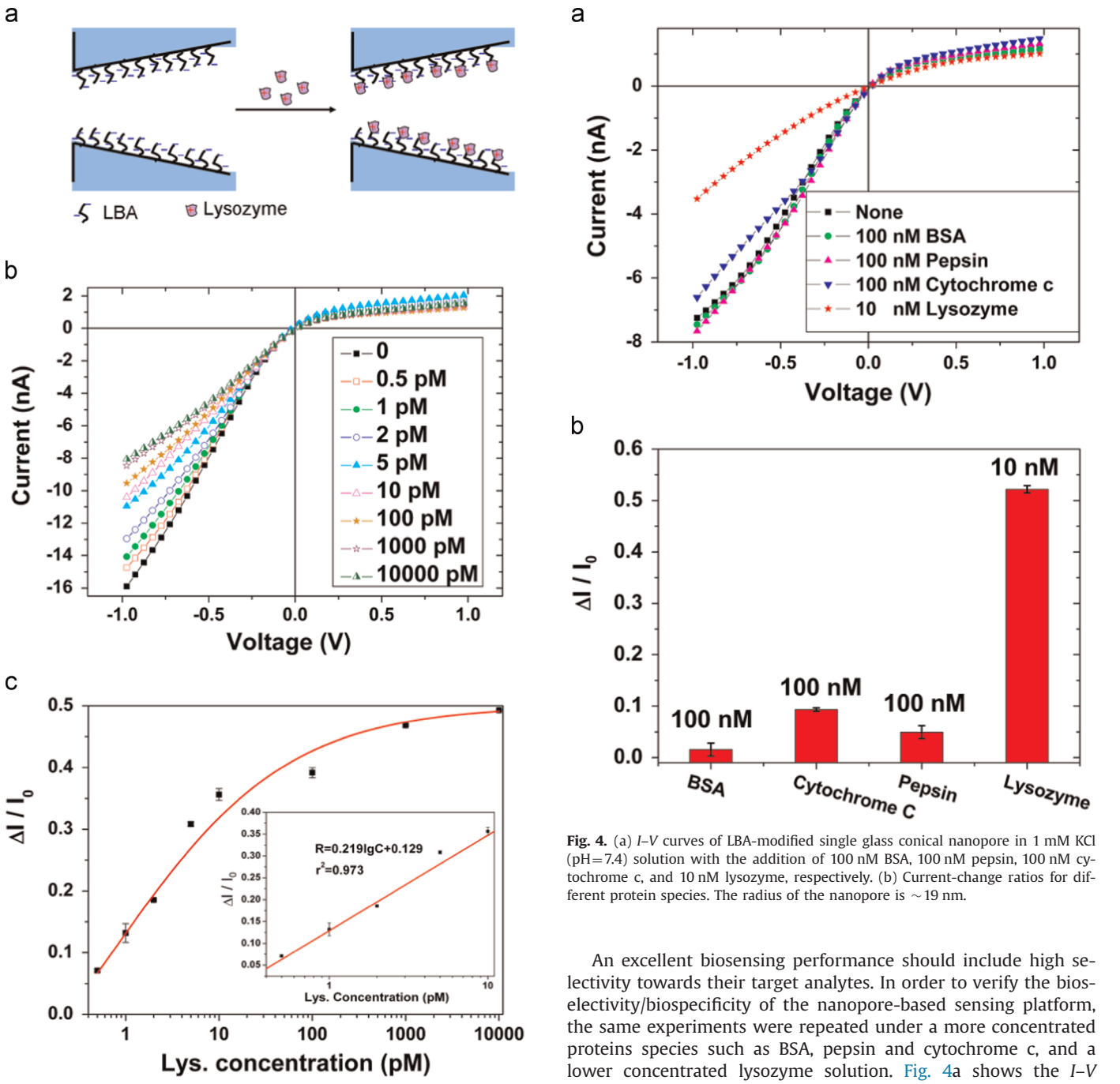

Fig. 3. (a) Schematic diagram of the biorecognition of lysozyme inside the nanopore channel. (b) *I–V* curves of the LBA-modified single glass conical nanopore in 1 mM KCl (pH=7.4) aqueous solution under the addition of various lysozyme concentrations. (c) The current-change ratio at −1 V versus the additional lysozyme concentrations. The inset describes the linear relationship between the current-change ratio and logarithm concentrations of lysozyme. The tip radius is ~20 nm.

experimental results above, our novel biosensing platform that combined conical nanopore channel and aptamer shows high sensitivity to the target analytes, with a detection limit down to 0.5 pM. It is worth mentioning that this concentration of lysozyme that we can detect is much lower compared with other methods based on the aptamer–protein interaction (Cheng et al., 2007; Peng et al., 2009; Rodriguez et al., 2005; Sener et al., 2010; Subramanian et al., 2013). We expect that it should benefit from the high susceptibility of the single conical nanopores towards the surface charge.

Fig. 4. (a) *I–V* curves of LBA-modified single glass conical nanopore in 1 mM KCl (pH=7.4) solution with the addition of 100 nM BSA, 100 nM pepsin, 100 nM cytochrome c, and 10 nM lysozyme, respectively. (b) Current-change ratios for different protein species. The radius of the nanopore is ~19 nm.

An excellent biosensing performance should include high selectivity towards their target analytes. In order to verify the bioselectivity/biospecificity of the nanopore-based sensing platform, the same experiments were repeated under a more concentrated proteins species such as BSA, pepsin and cytochrome c, and a lower concentrated lysozyme solution. Fig. 4a shows the *I–V* curves prior to and after exposing the LBA-modified nanopore to 100 nM BSA, pepsin, cytochrome c and 10 nM lysozyme solutions, respectively. There are merely slight changes in the ionic currents upon the addition of 100 nM BSA, pepsin or cytochrome c, due to the lack of binding capability of these control protein species towards the immobilized surface aptamer. However, when a lower concentration of lysozyme (10 nM) was treated with the same nanopore channel, a dramatical decrease in the ionic current (from ~7.3 nA to ~3.5 nA) was observed because of the specific aptamer–protein interactions occurred inside the nanopore surface. It should be noted that the cytochrome c had similar properties (with pI ~11, MW ~12 kDa) (Cheng et al., 2007; Margoliash and Smith, 1961, 1962) to those of lysozyme and was also positively charged under the electrolyte condition of pH=7.4. However, only a slight change from ~7.3 nA to ~6.6 nA of the ionic current were observed even in a higher concentration, indicating that the electrostatic interaction is not the dominant factor. We also

calculated the current-change ratio at −1 V when exposing the LBA-modified nanopore channel to different protein species. As seen from Fig. 4b, the addition of BSA, cytochrome c and pepsin just led to a decrease of ionic current with ~1.5%, ~9.3% and ~4.9%, respectively, but ~52% decrease occurred while treating with the lysozyme solution. These results indicated that the nanopore-based sensing system exhibited a remarkable selectivity and specificity towards lysozyme.

To demonstrate the reversibility of the nanopore-based aptasensor, a simple mild ultrasonication for 2 min in PBS solution was used to release the bound lysozyme molecules. This nanosensor was regenerated for at least 7 cycles without a noticeable loss of performance (see Fig. S2). In addition, we found that the LBA-modified single glass conical nanopore still had an excellent comparable response to the lysozyme molecules one month later (Fig. S3). This indicated the good durability of the nanosensor, which should be attributed to the superior robustness of glass-based nanopore and the stability of aptamer we used in this experiment.

3.3. Verification the essential role of aptamer

On the other hand, we further demonstrated that the protein analytes can only specifically bind with the aptamer immobilized on the inner pore walls, not with the other groups that generated in the modification process, such as silica hydroxyl groups, amino groups and aldehyde groups, and the non-specific DNA strands (with the sequence of 5′-NH_2-$(CH_2)_6$-ACT ATA CGT GCA TAT ACA GCT AGA GAT GCT AGG AGT ACT ATG-3′). For this purpose, negative control experiments were conducted in single glass conical nanopores that with silica hydroxyl groups, amino groups, aldehyde groups and Control DNA, respectively. Fig. 5 shows the *I–V* characteristics variations prior to and after the addition of 10 nM lysozyme in each modification step. As shown in Fig. 5, no significant changes were observed upon the addition of 10 nM lysozyme in each modification step even after 40 min incubation. Here we should notice that the unmodified and Control DNA-modified nanopore surfaces were negatively charged at pH=7.4 and it nearly did not respond to the positively charged lysozyme molecules. From all the results above, we demonstrated that the aptamer played a crucial role in specifically recognizing the target analytes when constructing a nanopore-based aptasensor.

3.4. Verification of the nanopore-based sensing strategy

We also conducted the same experiment in another two different nanopore channels functionalized with LBA (with radius of 10 nm and 15 nm, respectively). Fig. 6 shows the variation of current–voltage characteristics of the two different LBA-modified nanopore channels prior to and after the addition of 100 pM lysozyme. As expected, considerable decreases in ionic current of both the two nanopore channels (that is ~27% and ~54% decreases corresponding to channel 1 and channel 2, respectively) were observed due to the bioconjugation of the positively charged lysozyme molecules. These results further verified the feasibility of surface charge modulated nanopore biosensing strategy. We

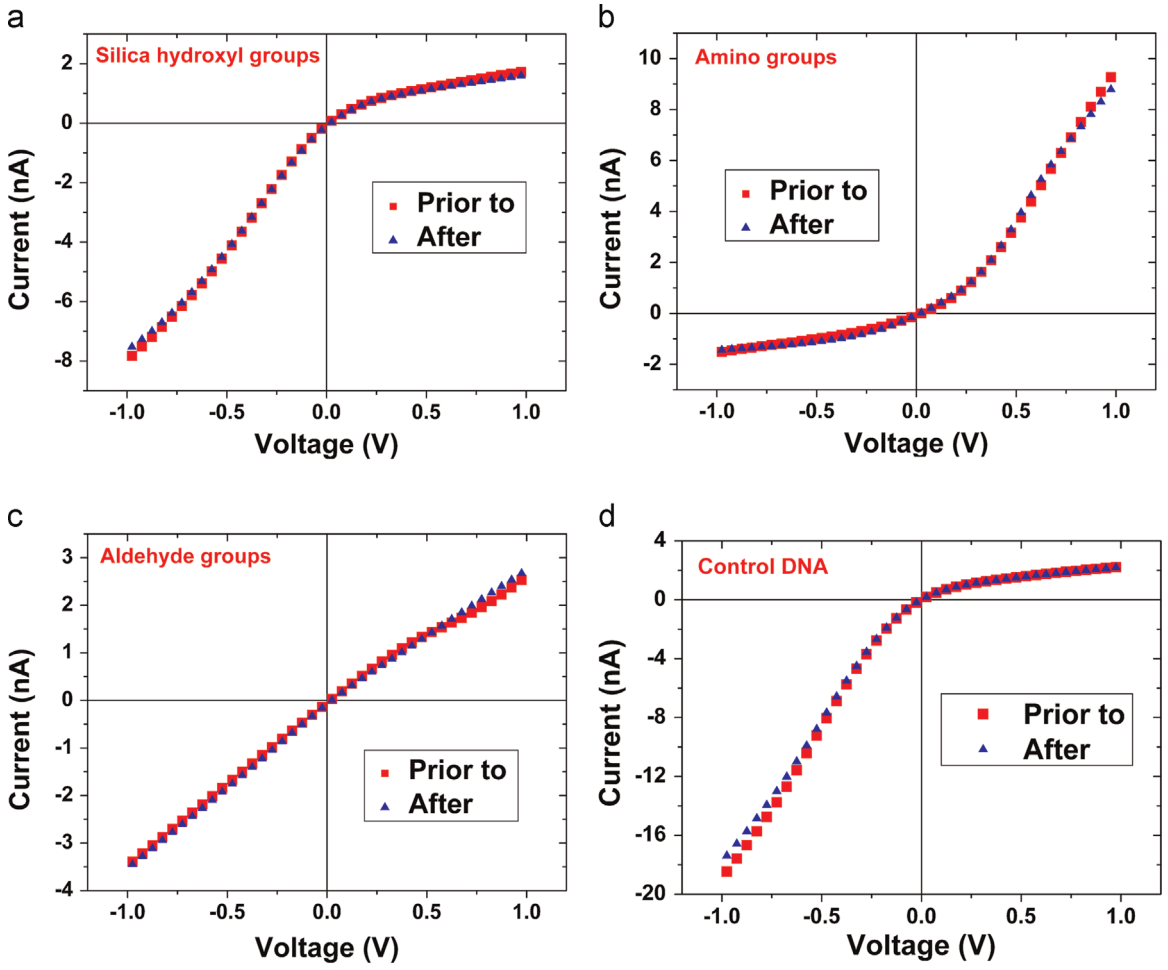

Fig. 5. *I–V* curves of a single glass conical nanopore in the 1 mM KCl (pH=7.4) solution prior to and after the addition of 10 nM lysozyme bearing (a) silica hydroxyl groups, (b) amino groups, (c) aldehyde groups, (d) non-specific DNA. The radius of the nanopore is ~10 nm.

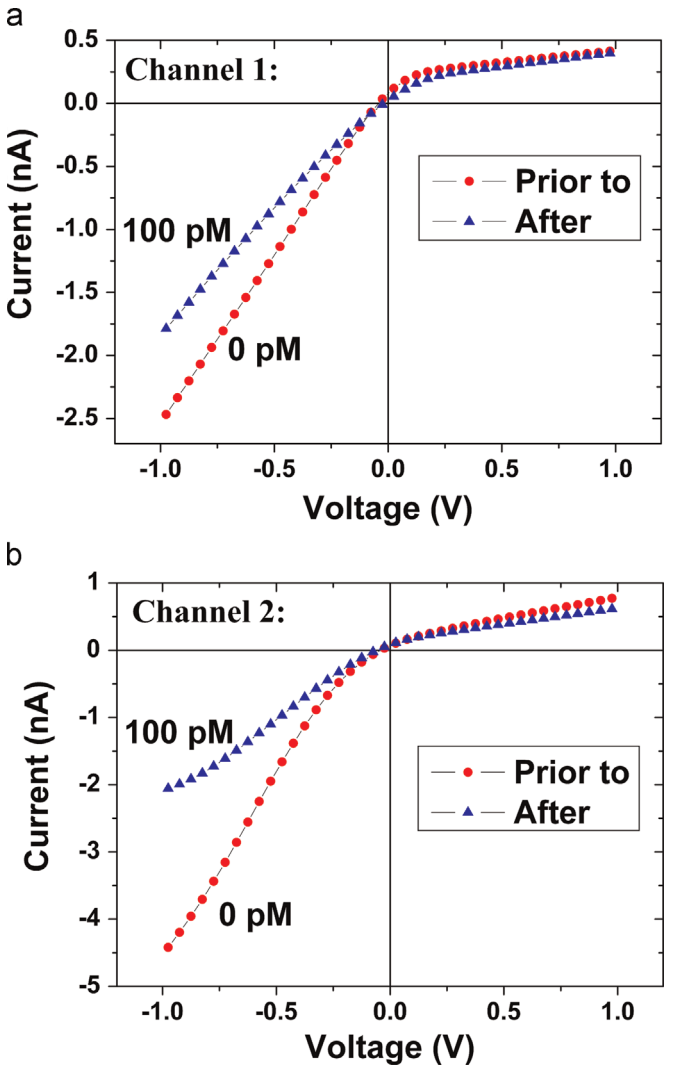

Fig. 6. *I–V* curves of LBA-modified single glass conical nanopore in 1 mM KCl (pH=7.4) solution having radius of (a) ~10 nm and (b) ~15 nm, prior to and after the addition of 100 pM lysozyme.

observed that the change in ionic current at $a=15$ nm (~54%) was larger than those at $a=10$ nm (~27%) and $a=20$ nm (~38%, Fig. 3). The difference of signal-change magnitude may result from the joint effects of pore sizes and surface charge. When the tip radius of the nanochannel is too small, the lysozyme molecules may not easily enter into the tip of nanochannel to react with LBA, which leads to a lower decrease in current change. However, too large pore size should have a smaller rectification effect even though the target molecules are easier to enter the tip side of the pore.

4. Conclusions

In summary, we have performed the DNA–protein interaction in a single glass conical nanopore and designed a novel label-free nanopore-based aptasensor for proteins. The negatively charged aptamers were covalently immobilized to the single glass conical nanopore wall through siloxane chemistry. Then, the lysozyme molecules in the solution were specifically recognized by the aptamer immobilized on the pore wall with high affinity, which neutralized the negatively charged walls and significantly reduced the ionic current. This novel nanodevice that combined the single glass conical nanopore with aptamer possessed the advantages of excellent high sensitivity, remarkable selectivity and reversibility, a reduction of materials consuming, and super robustness and stability. The limit of detection was 0.5 pM for target protein, which was a very low value compared to previous works. It only selectively responded to lysozyme but not to other protein species. Moreover, this strategy we described here can be readily extended to the detection of a wide range of protein targets if we control a proper pH condition to make sure there are opposite charge polarities between the protein molecules and corresponding aptamer.

Acknowledgments

We are grateful for the financial support from the National Natural Science Foundation of China (Grant nos. 21375111, 21127005 and 20975084), the 973 Program of China (2013CB933703), and the Fund of the Ministry of Education of the People's Republic of China (Grant no. 20110121110011, PCSIRT IRT13036).

Appendix A. Supplementary material

Supplementary data associated with this article can be found in the online version at http://dx.doi.org/10.1016/j.bios.2015.04.002.

References

Abelow, A.E., Schepelina, O., White, R.J., Vallee-Belisle, A., Plaxco, K.W., Zharov, I., 2010. Chem. Commun. 46, 7984–7986.
Actis, P., Rogers, A., Nivala, J., Vilozny, B., Seger, R.A., Jejelowo, O., Pourmand, N., 2011. Biosens. Bioelectron. 26, 4503–4507.
Ali, M., Nasir, S., Nguyen, Q.H., Sahoo, J.K., Tahir, M.N., Tremel, W., Ensinger, W., 2011. J. Am. Chem. Soc. 133, 17307–17314.
Ali, M., Nasir, S., Ramirez, P., Cervera, J., Mafe, S., Ensinger, W., 2012. ACS Nano 6, 9247–9257.
Ali, M., Neumann, R., Ensinger, W., 2010. ACS Nano 4, 7267–7274.
Ali, M., Yameen, B., Neumann, R., Ensinger, W., Knoll, W., Azzaroni, O., 2008. J. Am. Chem. Soc. 130, 16351–16357.
Cheng, A.K.H., Ge, B., Yu, H.Z., 2007. Anal. Chem. 79, 5158–5164.
Choi, Y., Baker, L.A., Hillebrenner, H., Martin, C.R., 2006. Phys. Chem. Chem. Phys. 8, 4976–4988.
Clarke, J., Wu, H.C., Jayasinghe, L., Patel, A., Reid, S., Bayley, H., 2009. Nat. Nanotechnol. 4, 265–270.
Ding, S., Gao, C.L., Gu, L.Q., 2009. Anal. Chem. 81, 6649–6655.
Dekker, C., 2007. Nat. Nanotechnol. 2, 209–215.
Fologea, D., Gershow, M., Ledden, B., McNabb, D.S., Golovchenko, J.A., Li, J.L., 2005. Nano Lett. 5, 1905–1909.
Fu, Y.Q., Tokuhisa, H., Baker, L.A., 2009. Chem. Commun., 4877–4879.
Gyurcsanyi, R.E., 2008. Trends Anal. Chem. 27, 627–639.
Harrell, C.C., Kohli, P., Siwy, Z., Martin, C.R., 2004. J. Am. Chem. Soc. 126, 15646–15647.
Hille, B., 1978. Biophys. J. 22, 283–294.
Hou, X., Guo, W., Jiang, L., 2011. Chem. Soc. Rev. 40, 2385–2401.
Hou, X., Guo, W., Xia, F., Nie, F.Q., Dong, H., Tian, Y., Wen, L.P., Wang, L., Cao, L.X., Yang, Y., Xue, J.M., Song, Y.L., Wang, Y.G., Liu, D.S., Jiang, L., 2009. J. Am. Chem. Soc. 131, 7800–7805.
Hou, X., Jiang, L., 2009. ACS Nano 3, 3339–3342.
Howorka, S., Siwy, Z., 2009. Chem. Soc. Rev. 38, 2360–2384.
Hucho, F., Schiebler, W., 1977. Mol. Cell Biochem. 18, 151–172.
Hurt, N., Wang, H.Y., Akeson, M., Lieberman, K.R., 2009. J. Am. Chem. Soc. 131, 3772–3778.
Kohli, P., Harrell, C.C., Cao, Z.H., Gasparac, R., Tan, W.H., Martin, C.R., 2004. Science 305, 984–986.
Krishnan, Y., Simmel, F.C., 2011. Angew. Chem. Int. Ed. 50, 3124–3156.
Lagerqvist, J., Zwolak, M., Di Ventra, M., 2006. Nano Lett. 6, 779–782.
Li, Y.-Q., Zheng, Y.-B., Zare, R.N., 2012. ACS Nano 6, 993–997.
Liu, N.N., Jiang, Y.N., Zhou, Y.H., Xia, F., Guo, W., Jiang, L., 2013. Angew. Chem. Int. Ed. 52, 2007–2011.
Luan, B.Q., Zhou, R.H., 2012. J. Phys. Chem. Lett. 3, 2337–2341.
Madampage, C.A., Andrievskaia, O., Lee, J.S., 2010. Anal. Biochem. 396, 36–41.
Margoliash, E., Smith, E.L., 1961. Nature 192, 1121–1123.
Margoliash, E., Smith, E.L., 1962. J. Biol. Chem. 237, 2151–2160.

Martin, C.R., Nishizawa, M., Jirage, K., Kang, M.S., Lee, S.B., 2001. Adv. Mater. 13, 1351–1362.
Niedzwiecki, D.J., Grazul, J., Movileanu, L., 2010. J. Am. Chem. Soc. 132, 10816–10822.
Peng, Y.G., Zhang, D.D., Li, Y., Qi, H.L., Gao, Q., Zhang, C.X., 2009. Biosens. Bioelectron. 25, 94–99.
Perozo, E., Cortes, D.M., Sompornpisut, P., Kloda, A., Martinac, B., 2002. Nature 418, 942–948.
Rodriguez, M.C., Kawde, A.N., Wang, J., 2005. Chem. Commun., 4267–4269.
Rotem, D., Jayasinghe, L., Salichou, M., Bayley, H., 2012. J. Am. Chem. Soc. 134, 2781–2787.
Savariar, E.N., Krishnamoorthy, K., Thayumanavan, S., 2008. Nat. Nanotechnol. 3, 112–117.
Schibel, A.E.P., Ervin, E.N., 2014. Langmuir 30, 11248–11256.
Sener, G., Ozgur, E., Yilmaz, E., Uzun, L., Say, R., Denizli, A., 2010. Biosens. Bioelectron. 26, 815–821.
Sexton, L.T., Horne, L.P., Sherrill, S.A., Bishop, G.W., Baker, L.A., Martin, C.R., 2007. J. Am. Chem. Soc. 129, 13144–13152.
Sexton, L.T., Mukaibo, H., Katira, P., Hess, H., Sherrill, S.A., Horne, L.P., Martin, C.R., 2010. J. Am. Chem. Soc. 132, 6755–6763.
Siwy, Z., Heins, E., Harrell, C.C., Kohli, P., Martin, C.R., 2004. J. Am. Chem. Soc. 126, 10850–10851.
Subramanian, P., Lesniewski, A., Kaminska, I., Vlandas, A., Vasilescu, A., Niedziolka-Jonsson, J., Pichonat, E., Happy, H., Boukherroub, R., Szunerits, S., 2013. Biosens. Bioelectron. 50, 239–243.
Tahir, M.N., Ali, M., Andre, R., Muller, W.E.G., Schroder, H.C., Tremel, W., Ensinger, W., 2013. Chem. Commun. 49, 2210–2212.
Tian, Y., Wen, L., Hou, X., Hou, G., Jiang, L., 2012. ChemPhysChem 13, 2455–2470.
Tian, Y., Zhang, Z., Wen, L.P., Ma, J., Zhang, Y.Q., Liu, W.D., Zhai, J., Jiang, L., 2013. Chem. Commun. 49, 10679–10681.
Wang, H.Y., Ying, Y.L., Li, Y., Kraatz, H.B., Long, Y.T., 2011a. Anal. Chem. 83, 1746–1752.
Wang, J., Martin, C.R., 2008. Nanomedicine 3, 13–20.
Wang, Y., Zheng, D.L., Tan, Q.L., Wang, M.X., Gu, L.Q., 2011b. Nat. Nanotechnol. 6, 668–674.
Wei, R., Gatterdam, V., Wieneke, R., Tampe, R., Rant, U., 2012. Nat. Nanotechnol. 7, 257–263.
Wu, H.C., Bayley, H., 2008. J. Am. Chem. Soc. 130, 6813–6819.
Xia, F., Guo, W., Mao, Y.D., Hou, X., Xue, J.M., Xia, H.W., Wang, L., Song, Y.L., Ji, H., Qi, O.Y., Wang, Y.G., Jiang, L., 2008. J. Am. Chem. Soc. 130, 8345–8350.
Xiao, Y.H., Wang, Y.P., Wu, M., Ma, X.L., Yang, X.D., 2013. J. Electroanal. Chem. 702, 49–55.
Yan, H., Xu, B.Q., 2006. Small 2, 310–312.
Ying, Y.L., Li, D.W., Liu, Y., Dey, S.K., Kraatz, H.B., Long, Y.T., 2012. Chem. Commun. 48, 8784–8786.
Yusko, E.C., An, R., Mayer, M., 2010. ACS Nano 4, 477–487.
Zhang, B., Zhang, Y.H., White, H.S., 2004. Anal. Chem. 76, 6229–6238.
Zhang, B., Zhang, Y.H., White, H.S., 2006. Anal. Chem. 78, 477–483.
Zhang, L.X., Cai, S.L., Zheng, Y.B., Cao, X.H., Li, Y.Q., 2011. Adv. Funct. Mater. 21, 2103–2107.
Zhang, L.X., Cao, X.H., Zheng, Y.B., Li, Y.Q., 2010. Electrochem. Commun. 12, 1249–1252.
Zhang, S., Bao, A., Sun, T., Wang, E., Wang, J., 2015. Biosens. Bioelectron. 63, 287–293.
Zhao, Q.T., de Zoysa, R.S.S., Wang, D.Q., Jayawardhana, D.A., Guan, X.Y., 2009. J. Am. Chem. Soc. 131, 6324–6325.
Zhao, S., Zheng, Y.B., Cai, S.L., Weng, Y.H., Cao, S.H., Yang, J.L., Li, Y.Q., 2013. Electrochem. Commun. 36, 71–74.